Eur. Polym. J. Vol. 26, No. 1, pp. 105–116, 1990
Printed in Great Britain

0014-3057/90 $3.00 + 0.00
Pergamon Press plc

KINETIC INHOMOGENEITY OF DIFFUSION AND SOLUBILITY OF GASES IN POLYMERS AT LOW TEMPERATURES

A. I. MIKHAILOV and S. I. KUZINA

Institute of Chemical Physics of the U.S.S.R. Academy of Sciences, Chernogolovka, Moscow Region, 142432, U.S.S.R.

(*Received* 28 *November* 1988; *received for publication* 2 *March* 1989)

Abstract—The processes of oxygen micro- and macrodiffusion in polystyrene have been studied, based on the oxidation of macroradicals and the rate of gas evolution from the polymer. The kinetic inhomogeneity of the system, evidently connected with the physical micro-inhomogeneity of the polymer matrix, is shown. For quantitative description of the kinetically inhomogeneous processes, a polychronous kinetic algorithm has been developed. It allows us to obtain the rate constants and distribution function of the activation energy and a pre-exponential factor. The polychronous character of the diffusion processes is mainly connected with a wide spectrum of activational barriers (~5 to 20 kcal/mol). The thermodynamic parameters of the process of oxygen dissolution in polystyrene have been determined.

INTRODUCTION

The rapid advances in the low-temperature chemistry and physics of polymers make data on the diffusion of gases into a polymer matrix at low temperatures very important for various branches of science and technology (the theory of diffusion, chemical kinetics, ageing and stabilization of polymers, medical sciences, biology, engineering, etc.). Most of the published data on diffusion processes in polymers refer to relatively high temperatures (300–400 K).

The present work aimed at studying low-temperature diffusion and solubility of gases (oxygen, argon) in a polymeric matrix. The experiments were carried out with polystyrene (PS). The diffusional displacement of gas molecules up to distances of 50–100 Å (an average distance between reactants) was determined from kinetic data on the oxidation reaction of macromolecules in photo-irradiated PS samples at 90–180 K [1]. The diffusion of species over such small distances in the absence of a concentration gradient is conventionally termed microdiffusion. The ordinary diffusion of gases in the presence of a concentration gradient (macrodiffusion) is studied by measuring the rate of the dissolved gas movement in the polymer within a temperature range of 130–350 K [2].

Chemical reactions and diffusion in polymers have their own special features because of restrictions put by the polymeric matrix on molecular mobility and by the structural inhomogeneity of a solid matrix. The accepted relationships of classical chemical kinetics are inapplicable to chemical reactions in the matrices. In the present work we report some new ideas of the so-called polychronous kinetics which accounts for the dispersion of kinetic parameters.

The experiments were performed with commercial atactic PS prepared by thermal polymerization (molecular mass $2 \cdot 10^5$, $\rho = 1.05\ g \cdot cm^{-3}$, $T_g = 80°C$). The samples were prepared in three modifications: powder with a particle size of 0.2 ± 0.1 mm; films of 25 μm thick; "lyophilized" (freeze-dried) PS with a surface area of about $185\ m^2\ g^{-1}$.

OXYGEN MICRODIFFUSION IN PS

Microdiffusion of O_2 molecules was studied by using the low-temperature oxidation of macroradicals in PS by monitoring the changes in their ESR spectra: $\dot{R} + O_2 \rightarrow R\dot{O}_2$. Free radicals were generated by u.v.-irradiation ($\lambda \leqslant 340$ nm) of PS powder at 77 K. The ESR spectra were taken with a standard 3 cm band radiospectrometer at SHF power of about 20^{-4} W.

Oxidation of radicals was performed by utilization of atmospheric oxygen dissolved in u.v.-irradiated powders under isothermal conditions upon stepwise temperature rise within the temperature range of 77–180 K. Upon equilibrium dissolution of air, the concentration gradient is absent, and O_2 molecules are uniformly distributed over the entire volume of a polymeric matrix. This eliminates macrodiffusion effects, and the migration of O_2 molecules toward free radical sites is due exclusively to microduffusion stages. This process represents a good model for studying diffusion-controlled reactions since O_2 molecules perturb the initial polymer matrix only slightly. Air solubility is *ca* 10^{19} molecules/g (g^{-1})* and hence the concentration of oxygen dissolved in PS is $[O_2] \simeq 2 \cdot 10^{18}\ g^{-1}$.

Upon low-temperature photolysis of PS, alkyl radicals ($R^{\cdot}$) are formed [3]. Heating of irradiated samples results in $R^{\cdot}$ oxidation, and alkyl radicals are quantitatively converted into peroxide radicals, the total concentration of radicals remaining constant up to 180 K ($[R^{\cdot}] + [RO_2^{\cdot}] =$ constant) [1]. During oxidation, the ESR spectra consist of superimposed

*Solubility was determined manometrically (see p. 107).

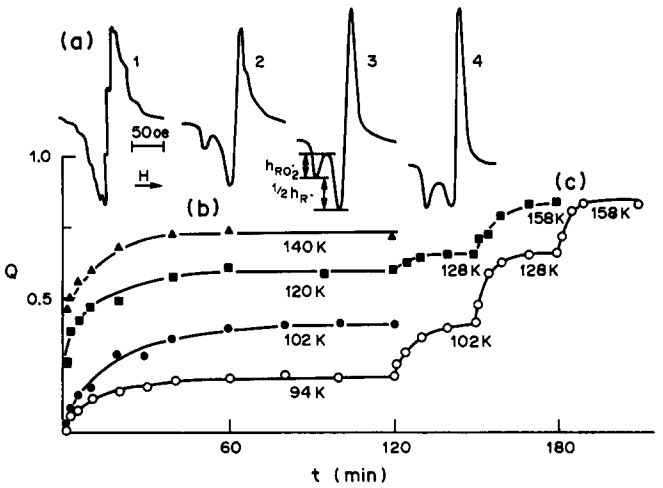

Fig. 1. (a) Changes in the ESR spectra of u.v.-irradiated PS as a function of Q: (1) $Q = 0$; (2) $Q = 0.3$; (3) $Q = 0.8$; (4) $Q = 1$. (b), (c) Kinetic curves of oxidation of macroradicals in PS.

signals from peroxide radicals $RO_2^{\cdot}$ (an asymmetrical singlet with anisotropic g factor) and from R$^{\cdot}$ radicals (Fig. 1a). The oxidation level may be expressed as

$$Q = [RO_2^{\cdot}]/([RO_2^{\cdot}] + [R^{\cdot}]) = h_{RO_2^{\cdot}} \times \beta_{RO_2^{\cdot}}/(S_{RO_2^{\cdot}} + S_{R^{\cdot}})$$

where $h_{RO_2^{\cdot}}$ is the amplitude of the low-field peak of the $RO_2^{\cdot}$ asymmetrical singlet. Shape factor $\beta_{RO_2^{\cdot}}$ can be found at $Q = 1$, i.e. upon complete oxidation of R$^{\cdot}$; $S_{RO_2^{\cdot}}$ and $S_{R^{\cdot}}$ are areas of the spectra of $RO_2^{\cdot}$ and R$^{\cdot}$, respectively. At $Q \geqslant 0.8$ it is more convenient to determine $S_{R^{\cdot}}$ as $S_{R^{\cdot}} = h_{R^{\cdot}} \times \beta_{R^{\cdot}}$ where $\beta_{R^{\cdot}} = S_{R^{\cdot}}/h_{R^{\cdot}}$ for $Q = 0$.

Previously it was shown [3] that radicals in PS are formed due to u.v.-irradiation ($\lambda \leqslant 340$ nm). Almost half of the radicals are produced in a layer 10 μm deep under the action of light with $\lambda = 240$–280 nm, i.e. within the region of the intrinsic absorption of PS. The remaining radicals are formed at $\lambda = 280$–340 nm at depths reaching 0.3 mm, i.e. larger than the size of the polymer powder particles. Therefore, the concentration of radicals both in the surface layer (*ca* 2×10^{17} g^{-1}) and in the bulk of PS powder (*ca* 0.5×10^{17} g^{-1}) is much smaller than that of dissolved oxygen ($[R^{\cdot}] \leqslant [O_2]$).

At 77 K, peroxide radicals are not produced in PS. However, at 90 K the ESR spectrum shows a low field $RO_2^{\cdot}$ component, i.e. the oxidation reaction begins. Under isothermal conditions, the rate of oxidation decreases sharply with time, the kinetic curves reach a plateau, and the reaction can be resumed only at a higher temperature. The extent of conversion for radicals in the plateau is a function of temperature, and independent of the way of sample heating (Fig. 1b, c). This phenomenon is typical of a variety of reactions in solid organic matrices and manifests itself not only in reactions where the diffusion-controlled nature is evident (stepwise recombination of radicals and their oxidation, solid phase polymerization [1, 4]) but also a number of "cage" processes [5]. The abrupt retardation of the process was named kinetic "stopping". It results from the kinetic inhomogeneity of the system when a wide range of chemically identical processes with different rate constants simultaneously occurs in a sample. These reactions (processes) may be conventionally termed "polychronous" as opposed to classical (monochronous) reactions described by a single rate constant. The kinetic inhomogeneity of the system can be related to the physical inhomogeneity of a solid body and to the effect of the surrounding on the molecular mobility of particles and the dynamics of the elementary act. In the case of "cage" reactions, the reason for the kinetic non-equivalence may be associated with the influence of the nearest neighbours on the interaction of the particles within the reaction volume. Hence, the inhomogeneity of the matrix may affect both the mobility of a particle and its chemical activity. In PS, kinetic stopping is specific to R$^{\cdot}$ oxidation not only in photo-irradiated samples [1] but also in γ-irradiated polymer [6] (where the distribution of the radicals within the sample is more uniform); the phenomenon manifests itself on consequent $RO_2^{\cdot}$ transformations [7].

Quantitative estimates show (see below) that the oxidation is controlled by the microdiffusion of O_2 molecules transport to the radical sites, provided that sufficient oxygen is dissolved in the polymer.

Thus, the processes of microdiffusion of O_2 molecules in PS at low temperatures are of a polychronous nature which seems to be related to the physical inhomogeneity of the polymer matrix, i.e. different regions of the polymer possess dissimilar rigidity and hence different molecular mobilities of the dissolved gas. The kinetics inhomogeneity of a sample should manifest itself in macrodiffusion processes also. In this context it was of interest to conduct a direct investigation of low-temperature diffusion of gases from the polymeric matrix proceeding from research on the microdiffusion step (by using the chemical reaction of R$^{\cdot}$ oxidation) to studies of the physical processes of diffusion and desorption.

MACRODIFFUSION AND THE MOVEMENT OF GASES DISSOLVED IN THE POLYMER

Macrodiffusion processes were studied by measuring the kinetics of movement of gas dissolved in PS.

The studies were carried out manometrically with the same samples of powdered polymer as used in the experiments on radical oxidation. Weighed amounts of polymer (*ca* 0.2 g) were placed in thin-walled silica cells, evacuated and saturated with the gas under investigation until equilibrium at the given temperature and pressure was reached. The cell was then quickly frozen by immersion in liquid N_2; the system was evacuated and joined to a manometer. Then it was thermostated at the required temperature. The system had a volume of about 3 cm^3. The temperature rise time of *ca* 2 min was taken into account in plotting the kinetic curves. The homogeneity of temperature distribution and the uncertainty in temperature did not exceed 2 K. Since the pressure of the gas was measured at different temperatures, appropriate corrections determined in control experiments have made. The results were reproducible within $\pm 5\%$.

At 77 K the gas evolution is insignificant (< 0.01 torr per hr); it increases at 130–140 K. Judging from the kinetics of R$^\cdot$ oxidation, the processes of microdiffusion of O_2 molecules into the bulk of the polymeric matrix are released to a considerable extent at this temperature and hence it is quite natural to relate gas evolution to the diffusion and desorption of the gas from the polymer. Control experiments showed that oxygen is not soluble in PS at 77 K, and O_2 molecules adsorbed on the surface of the sample are removed *in vacuo* which implies that their interaction with the surface becomes negligibly small.

Oxygen evolution from PS shows stepwise kinetics (Fig. 2a). In order to find out whether the isothermal retardation of the process is of a kinetic or a thermodynamic nature, we removed the gas evolved at a given temperature from the system. If the retardation of the process were of thermodynamic origin, then the shift in the equilibrium between sorption and desorption would lead to the evolution of the gas remaining in the polymer. However, no gas evolution at the given temperature was observed even when the sample was thoroughly evacuated. Nevertheless, at higher temperatures the process of gas evolution from the polymer continues (Fig. 2a for 171–197 K, 171–238 K, 238–300 K). Therefore, the observed retardation of the process does not result from the sorption/desorption equilibrium, but is of a kinetic nature.

Oxygen evolution from PS takes place over a wide range of temperature (130–350 K) (Fig. 3). These stepwise kinetics are observed not only for oxygen, for which specific interactions with matrix molecules might be expected, but also for such an inert gas as argon.

The usual formal kinetic relationships are unacceptable for the description of polychronous solid-phase processes. Consequently, a quantitative estimation of diffusional-kinetic parameters in the case of stepwise kinetics requires special consideration.

DETERMINATION OF THE KINETIC PARAMETERS OF POLYCHRONOUS PROCESSES

As noted above, the dynamics of the elementary act of solid-phase processes have particular features arising from strong restrictions to the molecular motions. Because of the slowing down, the time of the reaction (process) is not sufficient for the averaging of the kinetic inhomogeneity of the system by thermal motion, particularly at low temperatures. For a description of these processes, a broad spectrum of kinetic parameters with a certain distribution function for their values is to be introduced. At elevated temperatures, close to T_g or the melting temperature of the matrix, intense heat "mixing" averages out the distribution of kinetic parameters, and the process can be described by the usual equations of formal kinetics (as for gas/liquid systems).

The model of "polychronous" kinetics is promising and so far it is the only approach to a quantitative description of processes occurring in kinetically inhomogeneous systems. The model is based on the idea of a relation between the kinetic and physical inhomogeneity of the system. It is assumed that the ensemble of reacting species may be divided into groups where the process is characterized by rate constants from the interval of $(K, K + dK)$. At low temperatures, the "mixing" between these groups during the observation can be neglected. The overall kinetic curve consists of individual curves depicting the process in a certain elementary group of reactants. In the case of diffusional processes, this division of the reacting ensemble of species into groups is equivalent to the division of the matrix into separate regions ("zones") that can be characterized by "monochronous" diffusion coefficients. Similar views on the part played by inhomogeneities in a solid body have repeatedly been employed to account for certain physical phenomena, in particular the adsorption of gases on solid non-uniform surfaces [8], annealing of the electrical conductivity of metals [9], the population of the impurity levels in the photoconductivity of semiconductors [10], and carbon monoxide binding with mioglobin [11]. A quantitative description of the kinetics of low-temperature chemical reactions and diffusional processes in molecular solids and polymers can be found elsewhere [1, 2, 4]. The model of polychronous kinetics is not only applicable to thermally activated, but also to tunnelling, processes where the width of the barrier tunnelled by the reacting species (electron) acts as a distribution parameter [12].

Generally, the distribution of the reacting species with respect to rate constants may be due to the difference both in the activation energy, E, and in the pre-exponential, K_0 (or in E and K_0 simultaneously). As a rule, retardation of the process is observed when the width of the distribution of rate constants is of 5–10 orders of magnitude. In this process, the distribution parameters usually enter the rate constant in an exponential way, and it is therefore convenient to take ln K as the argument of the distribution function [8]. Let us assume that the reaction obeys the laws of conventional (monochronous) kinetics in the elementary "zone". Then, in the simplest cases of first and the second order reactions, $G_1 = \exp(-K_1 t)$ and $G_2 = (1 + n_0 K_2 t)^{-1}$, respectively. Thus, in order to obtain an overall kinetic expression, $n(t)$, we need to take the sum (integral) of the individual kinetic law, $G(K, t)$, for the kinetics of the process in the elementary "zone" over the entire sample for every moment of time t values and at a certain weight distribution

function, f(ln K):

$$n(t) = n_0 \int_{\ln K_{min}}^{\ln K_{max}} f(\ln K) G(K, t)\, d \ln K \qquad (1)$$

where n_0 and n are the initial and the current concentrations of the reactants and the range of rate constant values, K_{min}–K_{max}, characterizes the width of the distribution when the distribution function, f, differs from zero and satisfies the normalization condition:

$$\int_{\ln K_{min}}^{\ln K_{max}} f(\ln K)\, d \ln K = 1.$$

The general expression for the distribution function of kinetic parameters on the basis of experimen-

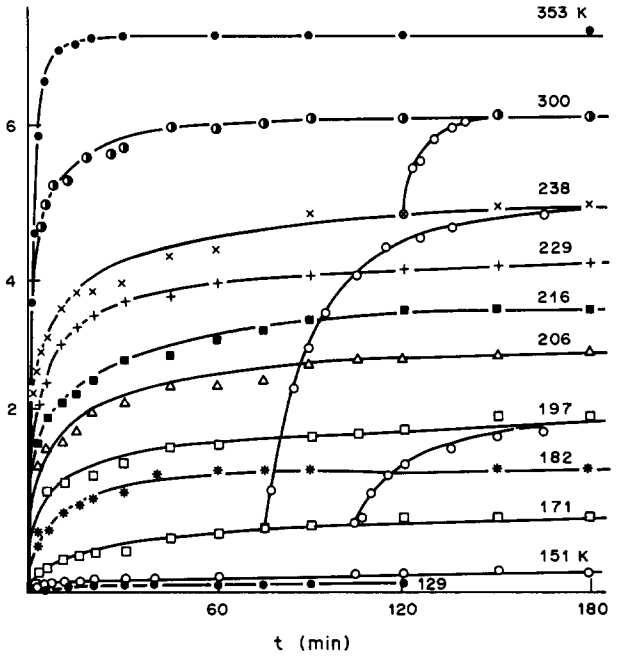

Fig. 2 (a). Kinetic curves of the evolution of oxygen dissolved at 300 K, 760 torr in PS powder.

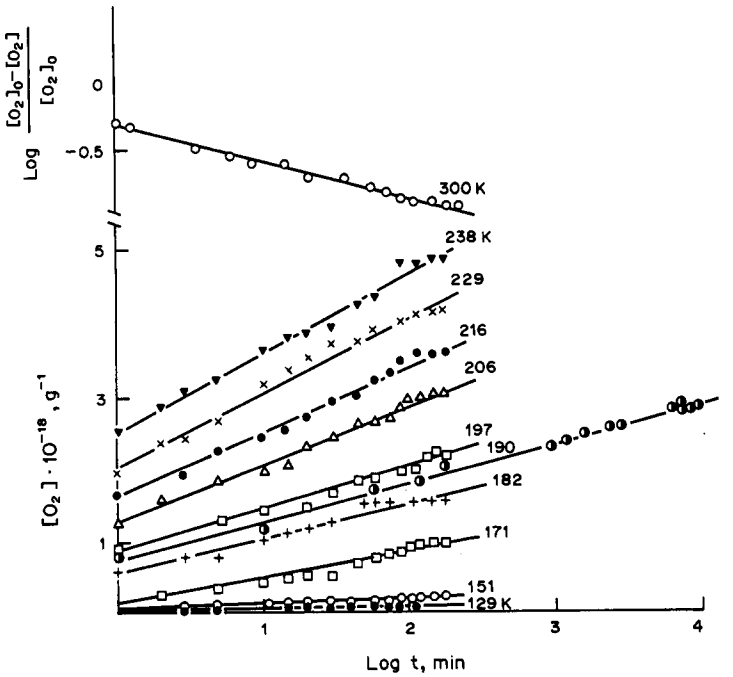

Fig. 2 (b). The transformation of the curves in $[O_2]$–log t coordinates; the coordinates for the 300 K curve are $\log([O_2]_0 - [O_2])/[O_2]_0 - \log t$ where $[O_2]_0 = 7 \times 10^{18}$ g^{-1} is the maximum amount of gas evolved from 1 g of the polymer.

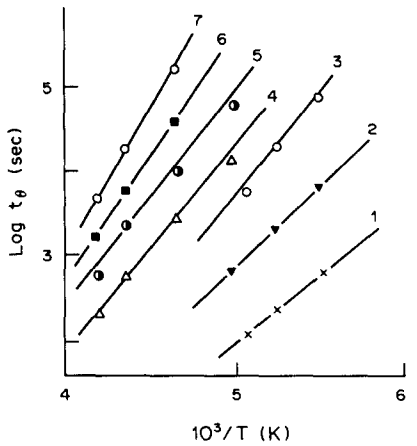

Fig. 2 (c). The Arrhenius dependence of the characteristic time, t_θ, obtained by the horizontal dissection of the kinetic curves $[O_2]$–log t at $\theta = [O_2]/[O_2]_0$ for θ values: (1) 0.14; (2) 0.21; (3) 0.28; (4) 0.42; (5) 0.50; (6) 0.57; (7) 0.65.

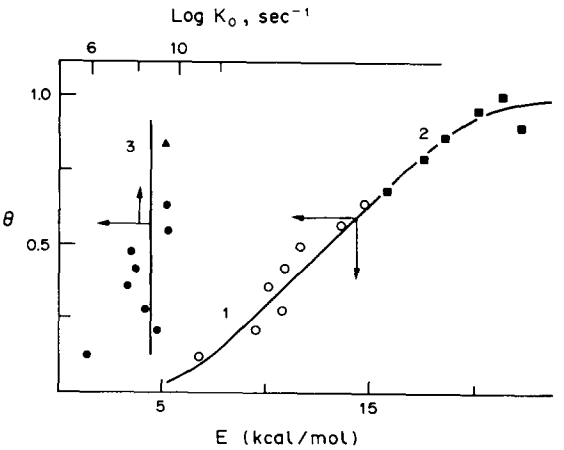

Fig. 2 (d). The integral distribution functions with respect to activation energies (1, 2) and the pre-exponential (3).

tal data may be obtained by solving the Fredholm integral equations of the first kind which represents a difficult mathematical problem not always soluble. Therefore, for some practically important G functions, an approximate analytical solution has been found.

In the case of the great isothermal retardation of the process, when K_{min} differs from K_{max} by 5–10 orders of magnitude and the dependence G(K) possesses some specific features (Fig. 4), we can substitute the Heaviside function for the G(K, t) function:

$$G_0(\ln K - \ln K^*) = \begin{cases} 1 \text{ at } K_{min} < K < K^* \\ 0 \text{ at } K_{max} > K > K^*. \end{cases}$$

The K^* value is found from the inflection point of the G(K) function and satisfies the condition $K_\alpha^* t = 1$ (Fig. 4), where for the first and second order reactions $\alpha = 1$ (for G_1) and respectively $\alpha = n_0$ (for G_2). With increasing time, the reaction front determined by the value of K^* shifts towards smaller values of the rate constant. The physical meaning of K^* is that at a certain moment, t, we can follow the kinetics of the process only for those species for which rate constants are within a narrow range near K^*. Species with larger rate constants ($K \gg K^*$) have already reacted and their concentration equals zero; on the other hand, species with small K values ($K \ll K^*$) have not yet reacted and their concentration equals the initial value. Thus, in expression (1) integration may only be carried out in the interval from ln K_{min} to ln K^* where G(K, t) = 1:

$$n(t) = n_0 \int_{\ln K_{min}}^{\ln K^*} f(\ln K)\, d \ln K. \qquad (2)$$

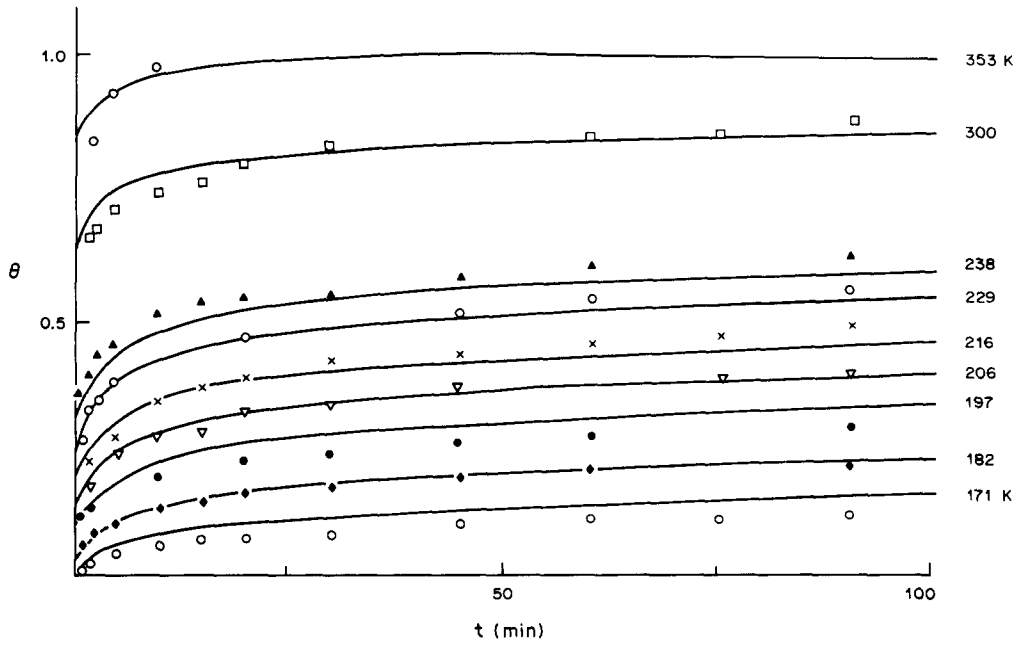

Fig. 3. Comparison of the simulated (——) and experimental data for oxygen evolution from PS in coordinates θ–t. The range of θ variation 0.2–0.98.

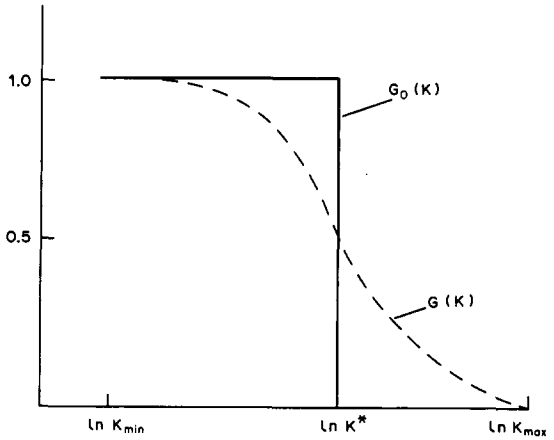

Fig. 4. The form of dependences $G(K)$ and $G_0(K)$.

Usually the distribution function is bell-shaped, and its central portion may be approximated by a "rectangular" function:

$$f(\ln K) = (\ln K_{max}/K_{min})^{-1} \times [G_0(\ln K/K_{max}) - G_0(\ln K/K_{min})]. \quad (3)$$

Then

$$n(t) = -n_0(\ln K_{max}/K_{min})^{-1} \ln K_{min}\alpha t. \quad (4)$$

If the activation energy E is a distribution parameter and $K_{max(min)} = K_0 \exp(-E_{min(max)}/RT)$, then:

$$n(t, T) = \frac{n_0}{E_{max} - E_{min}}(E_{max} - RT \ln K_0\alpha t). \quad (5)$$

Thus, in regions where $f(\ln K) \simeq$ constant, the retardation of the process is of a logarithmic nature, and the kinetic curves can be linearized in the n, $\log t$ coordinates. (It should be noted that the kinetic curves for first order monochronous processes give linear plots in the $\log n$, t coordinates.) At the wings of the distribution curve, the function $(n, \log t)$ is more complicated and may deviate from a straight line. Thus, in the case of the exponential dependence, the distribution function (which will be used below) has the form:

$$f(E) = A \exp[-(E_0 - E)/\Delta E] \quad (6)$$

where A, E_0 and ΔE are the parameters ($E \gg E_0$) and in accordance with equation (2):

$$n(t, T) = An_0 \exp^{E_0/\Delta E}(K_0\alpha t)^{-RT/\Delta E}. \quad (7)$$

Important information on the spectrum of rate constants of polychronous processes may be derived

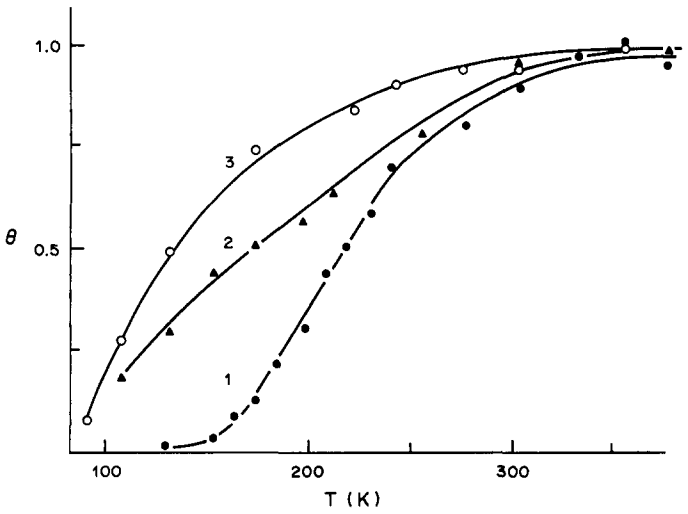

Fig. 5 (a). Gas evolution curves at stepwise heating: (1) PS powder (particle size 0.2–0.1 mm); (2) PS film (25 μm); (3) freeze-dried PS.

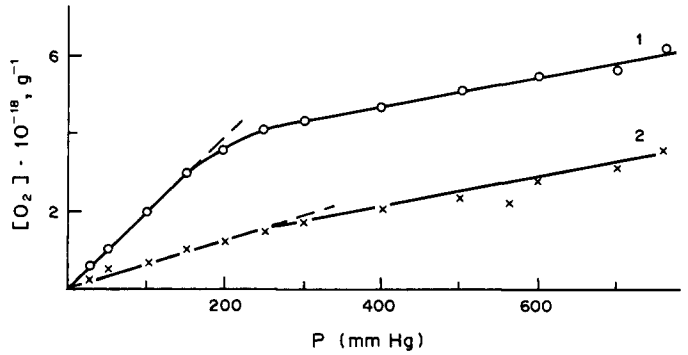

Fig. 5 (b). The dependence of O_2 solubility on oxygen pressure: (1) in PS; (2) in PMMA.

from the so-called "curve of stepwise heating", $n_{st}(T)$. The curve is obtained upon gradual heating followed by keeping for a certain period of time, τ, at a preset temperature until the concentration $n(\tau)$ is almost steady and $n(\tau) = n_{st}$. Since the n_{st} value does not depend on the way of sample heating (Figs 1b, c and 2a), the curve can also be obtained by vertical dissection of the family of kinetic curves at $t = \tau = \text{constant}$. In the case of distribution with respect to E, the stepwise heating curve directly reflects the shape of the integral distribution function

$$\theta = \int f(E)\,dE \text{ [1, 4]}. \tag{8}$$

Kinetic expressions $n(t)$ similar to equations (5)–(7) may also be obtained for the case when distribution occurs [12] with respect to the pre-exponential K_0.

The nature of the distribution parameter usually is not known *a priori*. Therefore, to analyse the temperature dependence of kinetic constants, to verify the applicability of the Arrhenius law, and to identify the nature of the distribution ("activational" or "pre-exponential"), we have developed the algorithm of polychronous kinetics based on the horizontal dissection of the family of kinetic curves $n(t, T)n_0^{-1} = \theta(t, T)$ at different levels of θ. Under condition (1a) of strong polychronousity, the kinetic curves $n(t, T)n_0^{-1} = \theta(t, T)$, according to equation (2), are the integral distribution function with respect to logarithm of characteristic times of a process in isokinetic zones. Here the characteristic times are the functions $t(\theta, T)$, inverse to the functions $\theta(t, T)$, that may be found from the horizontal dissection of the family $n(t, T)n_0^{-1}$.

In other words, a horizontal dissection of the family of kinetic curves $n(t, T)n_0^{-1}$ makes it possible to monitor at different temperatures the behaviour of species of the same "type" present in the same reaction "zone" where for all particles $K(\theta) \simeq$ constant, and to obtain the dependence of rate constant on T: $K(\theta, T_i) = t^{-1}(\theta, T_i)\alpha^{-1}$. Here $t(\theta, T_i)$ is the time at which the kinetic curve for the temperature T_i intersects a horizontal line $n_0^{-1}n(t, T) = \theta$. In fact, $K(\theta)$ is the common monochronous rate constant for the process in the elementary "zone" and a standard Arrhenius procedure can be applied. Having thus obtained a family of $K(\theta, T)$ at different θ values, we can (if the Arrhenius law holds) determine $E(\theta)$ and $\ln K_0(\theta)$ separately and hence directly determine the integral functions of distribution with respect to activation energy, $\theta(E)$, and to the pre-exponential, $\theta(\ln K_0)$, as inverse functions to $E(\theta)$ and $\ln K_0(\theta)$, respectively. It should be noted that if the monochronous kinetic curves of first and second order reactions are dissected in a similar way, the same value of activation energy E will be obtained for the whole family of Arrhenius dependences and the pre-exponential will be slightly ($\sim \ln \theta$) dependent on the level of the dissection.

Therefore, the solution of equation (1) is reduced to the solution of the functional equation $n(t, T) = \theta$ and finding the inverse function $\theta(K, T)$. Since the differentiation is known to be an incorrect operation leading to increased "noise", in the further discussion we shall restrict ourselves and search only for integral distribution function θ [but not for their differential forms $f(K, T)$].

The suggested algorithm makes it possible to approach the solution of inverse kinetic problem and to derive the main kinetic parameters for a number of polychronous processes in chemical and biological systems at low temperatures (oxidation of macroradicals and solid-state polymerization [2, 4], radical recombination in biopolymers [13, 14] and biological membranes [15, 16], technological process of cellulose extraction from wood [17]).

We shall illustrate the operation of the algorithm taking as examples the kinetics of the diffusion processes involved in gas evolution from the polymeric matrix of PS and the kinetics of low-temperature oxidation of macroradicals.

For a conventional monochronous model and a uniform initial spatial distribution of the concentration $[O_2]$, the amount of gas ($[O_2]$) emerging from the polymer is given* by:

$$[O_2] = [O_2]_0(1 - \exp^{-Kt}). \tag{9}$$

Upon rapid desorption from the surface

$$K = \frac{\gamma}{l^2} \cdot D = K_0 \exp(-E/RT) \tag{9a}$$

where D is the diffusion coefficient, and l is the diffusion pathway of the species, γ is the geometry factor (for a film, l stands for its thickness and $\gamma = \pi^2$). In view of the polychronous nature of the process, the expression for the overall kinetic curve will be similar to equation (1):

$$[O_2](t) = [O_2]_0 \left\{1 - \int_{\ln K_{min}}^{\ln K_{max}} f(\ln K)G(K, t)\,d \ln K\right\}. \tag{10}$$

Therefore, we may use this approach to discover diffusion kinetic parameters.

Indeed, the kinetic curves of oxygen evolution from PS can be linearized in the $[O_2]$, $\log t$ coordinates up to $t \simeq 160$ hr (Fig. 2b, 190 K). A horizontal dissection of the kinetic curves $[O_2](t, T)$ gives $K^{-1}(\theta, T)$ values which fall on a straight line in Arrhenius coordinates (Fig. 2c). Figure 2d shows the plots of $\theta(E)$ and $\theta(\log K)$. As is seen, when the concentration of $[O_2]$ changes within the range of θ values from 0.2 to 0.65 where the given family of kinetic curves needs the least extrapolation, the pre-exponential remains nearly constant and $\log K_0(\sec^{-1}) = 8.5 \pm 0.7$, while the activation energy varies between 9 and 15 kcal/mol. At temperatures >240 K, the curve of stepwise heating [Fig. 5a(1)], which reflects the behaviour of the integral distribution function, deviates from linear proportionality. This is related to the stronger (than logarithmic) retardation of the process. To evaluate the distribution function in the θ range 0.65–1.0, we made use of the high-temperature

*Strictly speaking, the $[O_2]$ concentration is given by the expression

$$[O_2] = [O_2]_0 \left\{1 - \frac{8}{\pi^2} \sum_{j=0}^{\infty} \frac{1}{(2j+1)^2} \cdot \exp[-(2j+1)^2 Kt]\right\},$$

while in equation (9) only the term with $j = 0$ is present. However, this results in the error of about several percent that could not be responsible for the observed kinetic stopping phenomena.

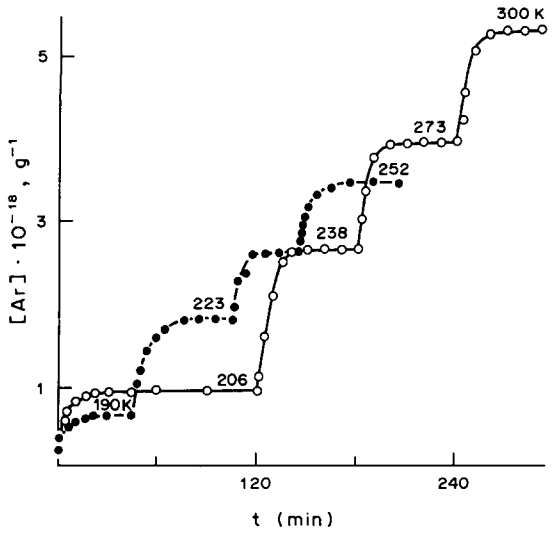

Fig. 6 (a). The kinetic curves of argon evolution from PS at 190–300 K.

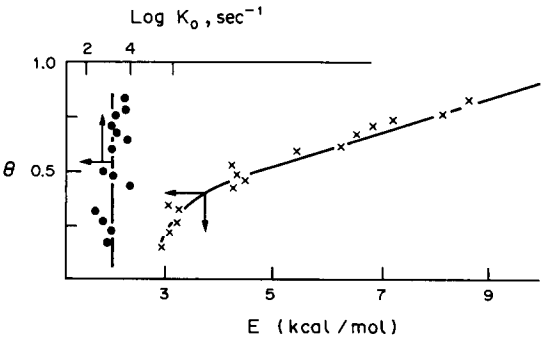

Fig. 6 (b). The integral distribution functions with respect to the activation energies and the pre-exponential for the process of O_2 evolution from PS film 25 μm thick.

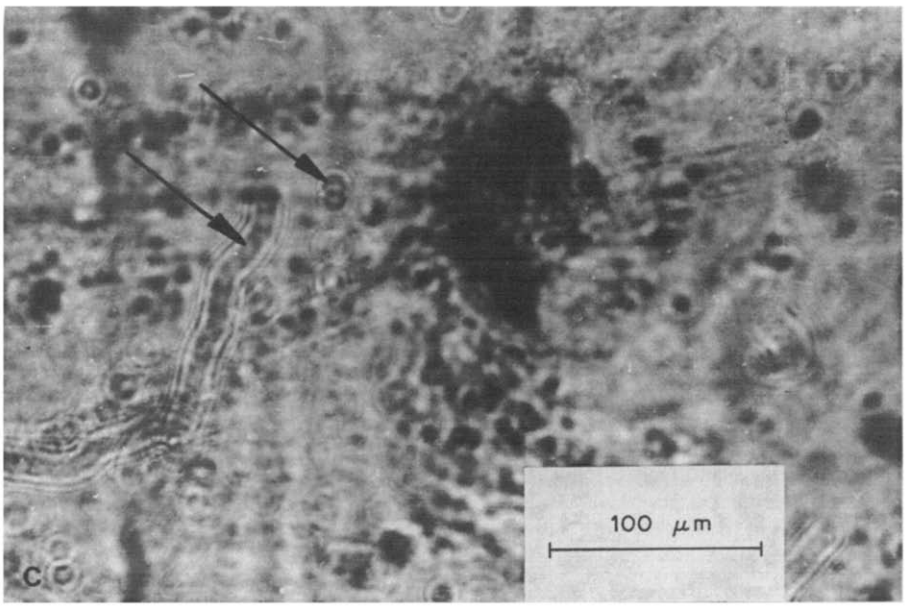

Fig. 6 (c). A photomicrograph of PS film (25 μm) after partial iodine desorption; exposure time in I_2 vapour at 280 K 30 days, time of desorption in air 2 days.

portion of the stepwise heating curve at $T =$ 240–350 K. Here we assume that $\log K_0 \simeq$ constant and the shape of the distribution function in this zone was approximated by an exponential law, $f(E) = A \exp[-(E_0 - E)/\Delta E]$. The kinetic curves should be given by relationship (7) and be linearized in the coordinates $\log [O_2]_0 - [O_2]/[O_2]_0$, $\log t$. The slope of these lines equals $RT/\Delta E$ and so ΔE may be found. The second portion of the distribution function $\theta(E)$ calculated as described above is shown in Fig. 2d (curve 2) and is seen to fit the low-temperature portion quite well; the value of $\log K_0(\sec^{-1}) -$ constant = 9 (point ▲ in the figure) almost coincides with the value of the pre-exponential determined earlier.

To compare experimental data with the values predicted by the algorithm of polychronous kinetics, expression (1) was used in computations.* Adequate simulation of the kinetic curves turned out to be feasible only when the experimental value of $\log K_0 \ll 9$ at $\theta = 0.1$ (cf. Fig. 2d, curve 3) was taken into account. The additional optimization of the solution resulted in satisfactory agreement between the theoretically predicted and experimental data at $E_{min} = 5$ kcal/mol, $E_{max} = 20$ kcal/mol and $\log K_0 =$ 4.7 at $1 < \theta < 0.3$ and $\log K_0 = 9$ at $\theta > 0.3$. The obtained approximate analytical solution to the in-

*The computations were carried out by O. V. Ushakovskii.

verse kinetic problem of polychronous kinetics provides the appropriate qualitative description of the experimental data (Fig. 3); the further optimization of this solution will certainly provide quantitative agreement.

Thus, the polychronous nature of the evolution processes of gas dissolved in the polymer is mainly associated with the distribution of the diffusion characteristics K with respect to activation energies. The distribution function $f(E)$ occupies the range from $E_{min} \simeq 5.5$ to $E_{max} \simeq 20$ kcal/mol (at $K_0 \simeq 3 \times 10^8$ sec^{-1}) and within the wide range may be readily approximated by a "rectangular" function where $\theta(E)$ is linear. It should be noted that for the initial portions of the curves ($t = 5$ to 10 min), the studies of N_2 evolution from PS [18] gave an activation energy of about 5.3 kcal/mol which is close to E_{min}.

The experiments on argon diffusion from PS powder (Fig. 6a) gave $E_{min} \simeq 10$ kcal/mol, $E_{max} \simeq 20$ kcal/mol, $K_0 \simeq 10^{10}$ sec^{-1}. The kinetic parameters of O_2 evolution from a PS film of uniform thickness (25 μm) were found as $K_0 \simeq 5 \times 10^3$ sec^{-1}, $E_{min} \simeq 3$ kcal/mol, $E_{max} \simeq 11$ kcal/mol; the plots of distribution functions, $\theta(E)$ and $\theta(\log K_0)$, are given in Fig. 6b.

Now consider the low-temperature oxidation of macroradicals in PS, the kinetics of which are also of a polychronous nature. In calculating the kinetic parameters of the raction

$$R^{\cdot} + O_2 \xrightarrow{K_{ox}} RO_2^{\cdot},$$

it may be assumed that, just as in the gas evolution processes, the pre-exponential $K_{ox}^0 = \text{constant}$ and variations in rate constants are related to the distribution of activation energies. In such a case, the distribution function obtained from the experimental curve of stepwise heating is of exponential type with the following values of the main kinetic parameters: $E_{min} \simeq 5.3$ kcal/mol, $E_{max} \simeq 12$ kcal/mol, $K_{ox}^0[O_2]_0 \simeq 2 \times 10^{10}$ sec^{-1} [1].

Before determining the nature (kinetic or diffusional) of the oxidation of macroradicals, we make the following points: (1) the rate of the oxidation and the kinetic parameters are independent of the identity of the radical undergoing oxidation. Thus, upon u.v. and γ-irradiation, different radical species are stabilized in PS [3]; however, in both the cases, the oxidation takes place within practically the same temperature range with close activation energies [1, 6], (2) the E_{min} values measured in the kinetic experiments on $R^{\cdot}$ oxidation virtually coincide with those determined for gas evolution. All this indicates that, during low-temperature oxidation of macroradicals, microdiffusion of oxygen molecules to the radical sites is the limiting stage and the measured rate constant K_{ox} is of a diffusional nature. From the expression for the rate constant of diffusion-controlled reactions, $K_{ox} = 4\pi r D_{micro}$ (r is the cage radius, $r \simeq 5$ Å), the microdiffusion coefficient D_{micro} may be found and the result compared with the macrodiffusion coefficients, D_{macro}, known from the literature. Thus, for O_2 diffusion in PS at 373 K, $D_{macro} \simeq 1.3 \times 10^{-6}$ cm^2 sec^{-1} [19]. On the other hand, noting that $K_{ox}^0[O_2]_0 = 2 \times 10^{10}$ sec^{-1} and $[O_2]_0 = 7 \times 10^{18}$ g^{-1} (Fig. 2a), we find that $K_{ox}^0 \simeq 3 \times 10^{-9}$ cm^3 sec^{-1}. Extrapolation of D_{micro} with the activation energy $E = E_{min} \simeq 5.5$ kcal/mol to the high temperature range gives D_{micro} (373 K) $\simeq 3 \times 10^{-6}$ cm^2 sec^{-1}. It is evident that D_{micro} is similar to D_{macro} in order of magnitude, supporting the conclusion on the diffusional nature of the oxidation reaction. The similarity between D_{micro} and D_{macro} also implies that in the processes of O_2 macrodiffusion, studied in the experiments on PS gas permeability [19], only migration of the gas along the "easiest pathway" is taken into account.

From the values of the pre-exponential, K_0, in the expression for the macrodiffusional rate constant, K, the diffusion path of the O_2 molecule may be estimated, i.e. the size of the diffusional "zone", l, where the diffusion coefficient, D, remains virtually constant. It follows from equation (9a) that

$$K = K_0 \exp(-E/RT) = \frac{\gamma}{l^2} D,$$

$$D = \tfrac{1}{6}\lambda^2 V_0 \exp(-E/RT) = D_0 \exp(-E/RT)$$

where λ is the length of the diffusion jump ($\lambda \simeq 5$ Å), V_0 is the frequency factor. Since $D_{micro} \simeq D_{macro}$, in evaluating the frequency factor, we can use the value of the pre-exponential in the expression for the rate constant of oxidation of the radicals by representing it as $K_{ox}^0 = V_0 v^*$. According to the experimental estimates [20], the reaction volume of radical reactions, v^*, is equal to *ca* 10^{-21} cm^3. The value of $V_0 = K_{ox}^0/v^* \simeq 3 \times 10^{12}$ sec^{-1} is in good agreement with frequencies of normal vibrations, i.e. in the elementary act of O_2 diffusion jump, the steric factor seems to be close to unity. Then, $D_0 = \frac{1}{6}\lambda^2 V_0 \simeq 10^{-3}$ cm^2 sec^{-1} (for N_2 diffusion in PS at 190–380 K, it was found that $D_0 \simeq 2 \times 10^{-4}$ cm^2 sec^{-1} [18]).

Thus, for PS powder $l \simeq 60\lambda \simeq 300$ Å and for PS film $l \simeq 15$ μm. Generally, for different PS samples, both the values of the activation barriers and the size of the "zone" evaluated from the frequency factor depend on the nature of the diffusing gas and the structure of polymer. As is seen, for a PS film of uniform thickness, l reaches the limiting value close to the geometric size of the sample (25 μm thick). Such large dimensions of the micro-inhomogeneities in the PS film made it possible to visualize these regions and to record them directly by using optical microscopy. For this purpose, we used iodine diffusion in PS, the iodine molecules causing intense yellow colouring. In the samples presaturated in I_2 vapours, the desorption of iodine molecules is more rapid from regions with maximum D values, while in the zones with small diffusion coefficients iodine is retained. The size of the micro-inhomogeneities determined by this method of visualization of polychronous zones in PS films is seen in Fig. 6c, the data being in good agreement with the values obtained in the experiments on oxygen diffusion.

The absolute value of the diffusion coefficient D_{macro} obtained from the kinetic parameters of the gas evolution process agrees with the D_{micro} value and the data available in the literature. Thus, D_{macro} ($E_{min} \simeq 5.5$ kcal/mol, 373 K) $\simeq 0.8 \times 10^{-6}$ cm^2 sec^{-1} which is close to the above-mentioned date [19]. D_{macro} (E_{min}) value conforms to the maximum figure

Table 1. O_2 Solubility in different PS samples (oxygen evolution at 300 K)

No.	Sample type	Treatment	O_2 (molecules/g)
1.	Pellets, 4 × 5 mm	—	*ca* 4×10^{18}
2.	Powder, grain size 0.2 mm	—	*ca* 6×10^{18}
3.	Film, 25 μm	—	*ca* 1×10^{19}
4.	Lyophilized PS, surface area ~185 m^2/g	—	*ca* 5×10^{20}
5.	Film, 25 μm	Heating at 400 K (0.5 hr)	*ca* 6×10^{18}
6.	Film, 25 μm	u.v. irradiation in air (253.7 nm; 2×10^{16} *quanta*/cm^2·sec; 236 K; 0.5 hr)	*ca* 5×10^{18}
7.	Film, 25 μm	γ-irradiation in air (300 M rad; 300 K)	*ca* 5×10^{18}

for the diffusion coefficient and characterizes, as noted above, the migration of gas molecules along the "easiest" pathway (i.e. the most defective and the least ordered sites of the polymeric matrix). The minimum value of the diffusion coefficient D_{macro} ($E_{max} \simeq 20$ kcal/mol, 373 K) is *ca* 3.1×10^{-15} $cm^2\,sec^{-1}$. It is evident that, because of the kinetic inhomogeneity of the polymeric matrix, the range for the coefficient amounts to several orders of magnitude. At low temperatures, the ratio D_{max}/D_{min} is even larger and reaches more than 30 orders of magnitude, e.g. at 100 K. It should be noted that the spread of K values caused by the scatter in the microscopic size of particles (Δl) of PS powder does not exceed one order of magnitude even at ($\Delta l = l = 0.2$ mm (powder grain size) and cannot account for such strong retardation of the process.

Thus, both the microdiffusion of O_2 molecules in the reaction of low-temperature R˙ oxidation and the macrodiffusion in the processes of low-temperature gas evolution from PS do not obey the laws of conventional "monochronous" kinetics. The phenomenon of kinetic stopping of the process is therefore observed, and it can be quantitatively described within the framework of the polychronous kinetic model. Such a stopping of the process is related to the kinetic inhomogeneity of the molecules at different sites in the polymeric matrix. The spectrum of kinetic parameters reflects the set of physical inhomogeneities existing in the real polymer. In this sense, examination of the diffusion of gases may provide a sort of "gas probe" method, furnishing information on the microstructure of a polymeric material.

SOLUBILITY OF GASES IN POLYMERS. DISSOLUTION ENTHALPY

Because of the polychronous nature of the low-temperature diffusion of gases in polymers, it was of interest to investigate the effects of the physical structure and micro-inhomogeneities of the polymeric matrix on the thermodynamic parameters of the dissolution process.

Table 1 presents data on oxygen solubility in various PS samples under equilibrium conditions at 760 Torr and 300 K. The O_2 concentration depends on the microstructure and preparation procedure of the sample increasing in the order: bulk PS/25 μm film/"lyophilized" PS. This observation is in accord with results obtained by Yakimchenko *et al.* [6] and may be used in studying various structural changes in the polymer. Thus, heating a particularly oriented PS film results in a lower oxygen solubility reaching that of bulk PS. The microstructure of a sample also affects the kinetics of gas evolution as may be seen from the gradual heating curves of three kinds of solid PS (Fig. 5a). The temperature of the onset of evolution of dissolved gas also decreases in the order bulk PS film/lyophilized PS, thus apparently indicating the imperfection of the microstructure. The same factor is likely to be responsible for lower E_{min} values (for bulk PS $E_{min} \simeq 5.5$ kcal/mol, for PS film $E_{min} \simeq 3.0$ kcal/mol).

Most of the available data on the solubility of gases in rubbers and other polymers have been obtained under normal conditions [21] with no attention to the prehistory of samples whereas the actual structure of a polymer composition can exert a substantial influence on the absolute values of the gas content.

The solubility of gases inert towards a polymer at pressures of about 1 atm is usually believed to obey Henry's law [22]. However, detailed studies revealed that the pressure dependence of O_2 solubility begins to deviate from proportionality at 200–300 Torr [e.g. for PS and poly(methyl methacrylate), Fig. 5b]. A similar dependence is also characteristic of sorption isotherms [23] for PS or poly(methyl methacrylate) in vapours of "inert" liquids.

The dependence of the solubility of gases in polymers on temperature usually has the form:

$$[O_2] = C_0 \exp(-\Delta H/RT) \qquad (11)$$

where C_0 is pre-exponential and ΔH is the dissolution enthalpy. At lower temperatures the equilibrium gas concentration in the polymer increases owing to the negative dissolution enthalpy. However, since the matrix is physically inhomogeneous and diffusion processes are of a polychronous nature, at limited dissolution times the equilibrium concentration is attained only in the "zones" (regions) of the polymer where the dissolution time, t_s, greatly exceeds the diffusion time ($t_s \gg l^2/D$). The rest of the sample remains practically inaccessible to the gas. Therefore, at lower dissolution temperatures, the amount of gas contained in the polymer only increases up to a certain limit and then starts falling because the region of the polymeric matrix accessible to gas saturation at a given temperature becomes smaller. Strictly, the equilibrium saturation of PS with gas at a limited dissolution time can only be achieved at temperatures higher than that of the complete gas evolution from the polymer. For PS, this is the range 330–350 K which is close to T_g.

Figure 7a shows the plots of O_2 evolution as a function of temperature of complete gas discharge during the gradual heating of PS powder samples

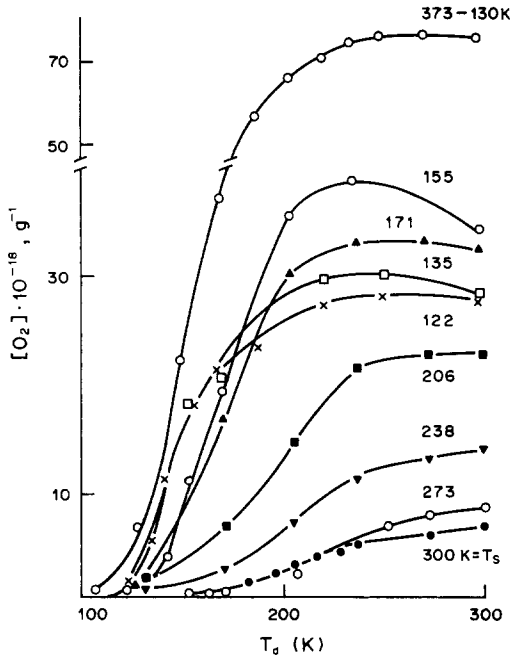

Fig. 7 (a). Gas evolution curves from PS powder when samples saturated with gas at different dissolution temperatures were gradually heated.

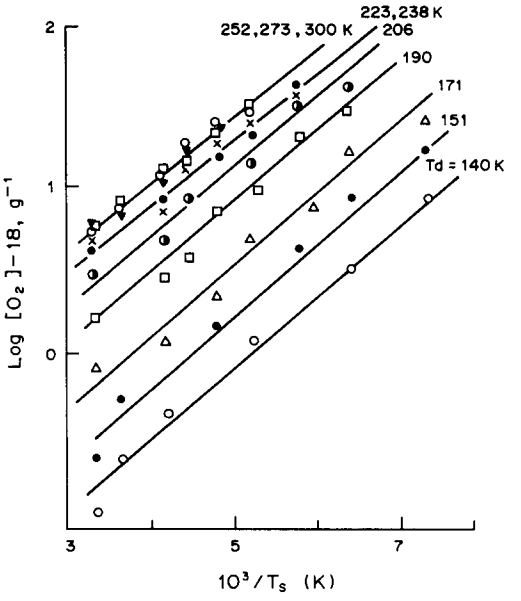

Fig. 7 (b). Arrhenius plot $\log[O_2] - 1/T$ for different "zones" of a sample obtained along the vertical dissection of the curves (a).

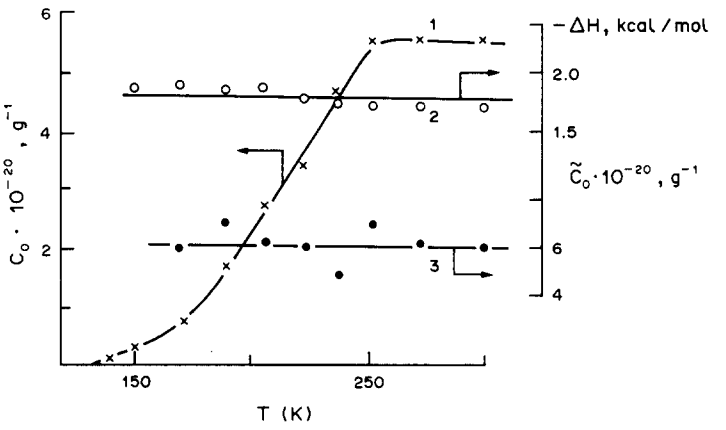

Fig. 7 (c). The dependence of the pre-exponential, C_0, (1), dissolution enthalpy ΔH (2), and the concentration of the centres capable of sorption, $\tilde{C}_0$, (3) on the temperature of gas discharge.

saturated with the gas at different temperatures. The gas saturation time of the samples at a given temperature was 2 hr; as reference experiments show, a twofold increase in the saturation time does not lead to any rise in the amount of sorbed gas. Hence, the zones of the polymeric matrix accessible to the gas were almost saturated to equilibrium concentration during the saturation time. It can be seen that at first the gas content grows as the dissolution temperature drops to *ca* 155 K; after that, the gas content starts falling and, as was noted earlier, at the temperature of liquid nitrogen, oxygen virtually does not dissolve in PS. It should be mentioned that the largest concentration of the gas can be obtained during the slow cooling of the sample when equilibrium sorption conditions are maintained throughout the entire period of time. Thus, at a cooling rate of *ca* $0.2\ K \cdot min^{-1}$ within the range of 373–130 K, a PS sample dissolves up to $7.5 \times 10^{19}\ g^{-1}$ which is an order of magnitude more than for dissolution under normal conditions (Fig. 7a, curves for 373–130 and 300 K).

On the basis of the observed wide range of activation energies of the diffusion characteristics at low temperatures, we might expect that dissolution enthalpy is also of a polychronous nature. In order to examine this problem and to obtain values of ΔH and the pre-exponential C_0 for different "zones" of the sample, we had to compare solubilities not only at different dissolution temperatures, T_s (which is often

done in determining ΔH) but also at different gas evolution temperatures, T_d.

Consider Fig. 7a; a vertical section of this family of curves at a given observation temperature, T_d, makes it possible to monitor the amount of gas in a chosen "zone" and to obtain the T_s dependence of the solubility in the polymer regions accessible to O_2 at a chosen T_d value. This dependence of oxygen concentration, $[O_2]$, on T_s at a constant gas discharge temperature, T_d, can be represented as a linear plot in Arrhenius coordinates except for portions where T_d is much higher than T_s (Fig. 7b). The values obtained for the dissolution enthalpy are similar for all the "zones" of the polymer sample, independent of the gas discharge temperature, T_d, in the range 140–300 K, and equal to $\Delta H = -1.8 \pm 0.1$ kcal/mol [Fig. 7c (2)]. This ΔH value is typical of the processes of physical sorption of gases in polymers including rubbers [21]. Where there is a strong interaction (of chemisorption type) between the gas molecules and a solid sorbent, the adsorption heat varies over a wide interval, the highest ΔH values being observed at the initial moments when the surface is saturated with gas [8]. It is noteworthy that the generally accepted methods of determining dissolution enthalpy comprise gas saturation of a sample at different temperatures and solubility measurement at a single temperature, usually 300 K. In the family of plots in Fig. 7b, the dependence for 300 K also giving the enthalpy value of -1.8 kcal/mol corresponds to the method of enthalpy calculation mentioned above.

The pre-exponential C_0 in expression (11) for gas solubility represents the number of centres capable of sorption in 1 cm^3 of a substance. Taking the inhomogeneity of the polymer matrix into account, we can express C_0 as a product of concentration of these centres ($\tilde{C}_0$) and the volume of "zones" (v) accessible to gas saturation at a given temperature:

$$C_0 = \tilde{C}_0 v(T). \tag{12}$$

The temperature dependence of C_0 is represented in Fig. 7c(1). To explain this dependence, it should be noted that the function $v(T)$ in expression (12), just like the gradual heating curve, $\theta(T)$, is associated with the inhomogeneity of the system and should reflect the shape of the distribution function of the diffusion parameters with respect to activation energies. Figures 5a and 7c(1) show that the $C_0(T)$ and $\theta(T)$ dependences are similar. Then in equation (12), $\theta(T)$ can be substituted for $v(T)$ giving: $\tilde{C}_0 = C_0(T)/\theta(T) \simeq 6 \times 10^{20}\,\mathrm{g}^{-1} = \text{constant}$ at θ from 10 to 90%, i.e. the concentration of the sorption centre in the entire volume of the sample is the same. The value of $\tilde{C}_0$ can be compared to the number of structural unit cells, N_0, in 1 cm^3 of PS

$$N_0 = N_A/MZ \simeq 6 \times 10^{20}\,\mathrm{cm}^{-3}.$$

Here, N_A is the Avogadro number, M is the molecular mass of a structural unit of the PS macromolecule (*ca* 100), Z is the coordination number ($Z \simeq 10$). The coincidence of $\tilde{C}_0$ with N_0 may well show that virtually every structural unit cell of PS can serve as a centre of sorption.

Thus, the diffusion processes of low-temperature gas evolution feature a wide range of the activation energies. Dissolution enthalpy as a thermodynamic characteristic of the system and the concentration of centres capable of sorption are practically the same for all the "zones" of the polymer sample and conventional thermodynamic relationships for the dissolution process remain true.

REFERENCES

1. A. I. Mikhailov, S. I. Kuzina, A. F. Lukovnikov and V. I. Goldanskii. *Dokl. Akad. Nauk SSSR* **204,** 383 (1972).
2. S. I. Kuzina and A. I. Mikhailov. *Dokl. Akad. Nauk SSSR* **231,** 1395 (1976).
3. S. I. Kuzina, A. I. Mikhailov and V. I. Goldanskii. *Int. J. Radiat. Phys. Chem.* **8,** 503 (1976).
4. A. I. Mikhailov, Ya. S. Lebedev and N. Ya. Buben. *Kinet. Katal.* **5,** 1020 (1964); *ibid.* **6,** 48 (1965); A. I. Mikhailov, A. I. Bolshakov, Ya. S. Lebedev and V. I. Goldanskii. *Fizika tverd. Tela* **14,** 1172 (1972).
5. N. M. Emanuel, W. A. Roginskii and A. L. Buchachenko. *Usp. Khim.* **51,** 361 (1982).
6. O. E. Yakimchenko, I. S. Gaponova, V. M. Goldenberg, G. V. Pariiskii, D. Ya. Toptygin and Ya. S. Lebedev. *Izv. Akad. Nauk SSSR, ser. Khim.* **1974,** 354.
7. V. A. Radtsig and M. M. Rainov. *Vysokomolek. Soedin* **A18,** 2012 (1976).
8. Ya. S. Zeldovich. *Acta Physicochim. URSS* **1,** 961 (1935); S. Z. Roginskii. *Izd. Akad. Nauk SSSR* **M.-L.,** 1948.
9. W. Primak. *J. appl. Phys.* **31,** 1525 (1960).
10. A. Rose. Fundamentals of the photoconductivity theory (Russian translation). Mir, Moscow, 1966.
11. R. H. Austin, K. W. Besson, I. Eisenstein, H. Frauenfelder and I. S. Gunsalus. *Biochemistry* **14,** 5355 (1975).
12. A. I. Mikhailov and V. A. Anikolenko. *Dokl. Akad. Nauk SSSR* **230,** 102 (1976).
13. O. V. Plotnikov, A. I. Mikhailov and E. L. Rayave. *Vysokomolek. Soedin* **A19,** 2528 (1977).
14. V. I. Devkin and A. I. Mikhailov. *Biofizika* **23,** 775 (1978).
15. V. G. Omelyanenko, A. I. Mikhailov, G. R. Kalamkarov, M. A. Ostrovskii and V. I. Goldanskii. *Dokl. Akad. Nauk SSSR* **273,** 1498 (1977).
16. V. I. Goldanskii, A. I. Mikhailov, V. G. Omelyanenko, V. N. Smirnov and V. P. Torchilin. *J. Lipid Res.* **22,** 131 (1981).
17. A. I. Mikhailov, V. I. Goldanskii, O. V. Plotnikov, L. P. Belkova and V. S. Gromov. *Fourth Int. Symp. Wood Pulping Chem.*, Paris, April 27–30 **2,** 69.
18. V. A. Tochin and D. N. Sapozhnikov. *Vysokomolek. Soedin* **A16,** 605 (1974).
19. T. K. Kwei and N. M. Arnheim. *J. Polym. Sci.* **A2,** 957 (1964).
20. A. I. Mikhailov, I. I. Migunova, V. S. Ivanov, I. M. Barkalov and V. I. Goldanskii. *Vysokomolek. Soedin* **A18,** 1226 (1976).
21. S. A. Reitlinger. *Pronitsaemost' polimernykh materialov* (Permeability of Polymeric Materials). Khimiya, Moscow, 1974.
22. D. W. Krevelen. *Properties of Polymers Correlations with Chemical Structure.* Elsevier, Amsterdam (1972).
23. A. A. Tager and M. V. Tsilipotkina. *Usp. Khim.* **47,** 152 (1978).